EOS, TRANSACTIONS, AMERICAN GEOPHYSICAL UNION

EOS

VOLUME 76 NUMBER 1

JANUARY 3, 1995

PAGES 1–8

Sonic Imaging Reveals New Plate Boundary Structures Offshore New Zealand

PAGES 1,4–5

J.-Y. Collot, J. Delteil, R. H. Herzer, R. Wood, K. B. Lewis, and Shipboard Party

Recent bathymetry and sonar imagery studies of offshore portions of the plate boundary transecting New Zealand allow the first confident mapping of detailed tectonic and sedimentary patterns of the region. Working in late 1993 aboard the R/V *L'Atalante* of the Institut Francais de Recherche pour l'Exploitation de la Mer (IFREMER), we recorded soundings of a wide swath of seabed to elucidate major structural transitions along the plate boundary. Results of the study, part of the GEODYNZ-SUD program developed jointly by institutions in France and New Zealand, will be complemented by New Zealand cruises to the Puysegur and Hikurangi margins. The total data set will be processed and interpreted during the next two years.

A shipboard SIMRAD EM12Dual (EM12D) multibeam system recorded 160,000 km^2 of swath bathymetry and imagery over the Kermadec-Hikurangi margin to the northeast and the Fiordland-Puysegur margin to the southwest of New Zealand (Figure 1). The EM12D consists of separate multibeam echosounders, each generating 81 stabilized beams at frequencies of 12.6–13 kHz. This system allows simultaneous determination of 162 measurements of phase giving depth and 162 measurements of the energy back-scattered. After on-board processing, swath maps of bathymetry and side scan sonar imagery over a maximum 22 km-wide strip of seabed were produced for each survey line. Swath data were augmented by geopotential data and six-channel seismic reflection data shot with two 75 cu in SODERA GI guns.

J.-Y. Collot, Institut Francais de Recherche Scientifique pour le Developement en Cooperation, Villefranche s/mer, France; J. Delteil, Institut de Geodynamique, Nice, France; R. Herzer and R. Wood, Institute of Geological and Nuclear Sciences; and K.W. Lewis, National Institute of Water and Atmospheric Research, Wellington, New Zealand

The active margins of New Zealand reflect complex temporal and spatial interactions between subduction and strike-slip regimes along the Pacific-Australian plate boundary. Because the PAC-AUS pole of rotation for this plate boundary lies to the southeast (60.1°S, 178.3°W) [*De Mets et al.*, 1990], the high-angle convergence along the Kermadec Trench changes to oblique convergence of opposite polarity along the Puysegur Trench (Figure 1).

Between the trenches, the plate boundary crossing the New Zealand continental crust is characterized by strike-slip and compressive (i.e., transpressive) deformation along the Alpine Fault (Figure 1). On the GEODYNZ-SUD cruise we studied the variations in deformation and sedimentation associated with changes from oceanic subduction to intra-continental transpression. The following observations were among the highlights:

- widespread tectonic erosion along the northern Hikurangi-Kermadec margin caused by the collision of ridges and volcanic seamounts;
- extensive offshore strike-slip faulting along segments of the Hikurangi-Kermadec margin;

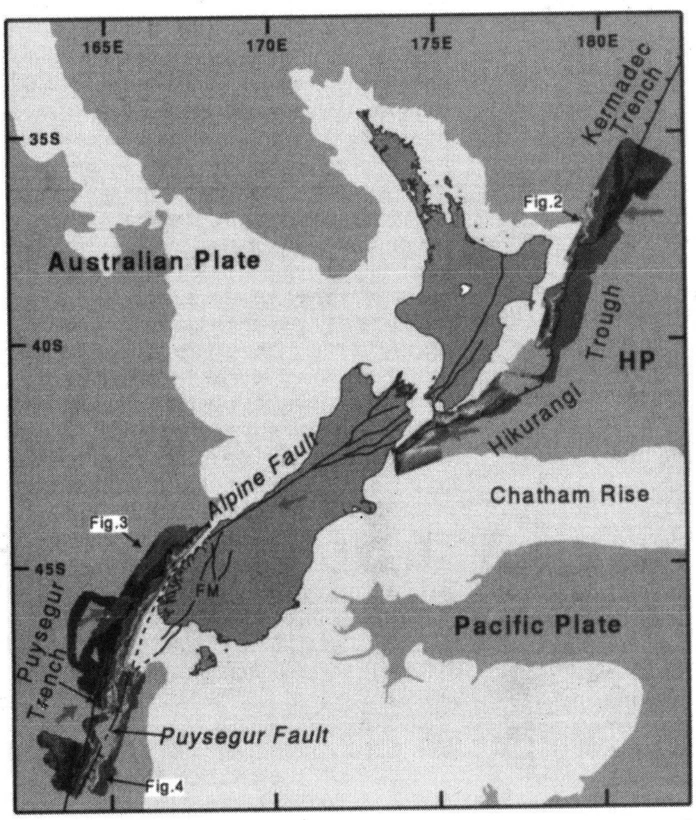

Fig. 1. Map of the areas surveyed during the Geodynz-Sud cruise of the R/V L'Atalante *along New Zealand's active margins with linearly color-coded swath bathymetry; red arrows = PAC-AUS plate convergence direction* [De Mets et al., 1990]; *HP = Hikurangi Plateau; FM = Fiordland Margin; sawtooth lines = subduction fronts; heavy lines = major strike-slip faults; light blue = continental rocks, depth <1.5 km; and dark blue = seafloor depth >1.5 km. Original color image appears at the back of this volume.*

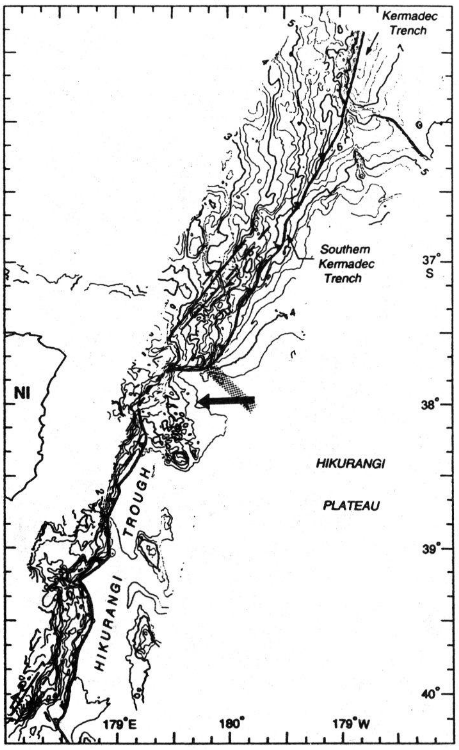

Fig. 2. Generalized multibeam bathymetric map (contour interval 250 m) of the northern Hikurangi-Kermadec margin showing the uplifted, en echelon southern Kermadec trench, the indented northern Hikurangi margin and the location of strike-slip deformation; sawtooth line = subduction front; large arrow = PAC-AUS plate convergence direction; shaded zone = ridge damming the sediment of the Hikurangi Trough; and NI = North Island.

- a ridge forming a dam that prevents movement of turbidity from the Hikurangi Trough to the Kermadec Trench
- a major strike-slip fault zone extending along the summit of the Puysegur Ridge (the Puysegur Fault);
- a relay zone of splay faults linking the Alpine Fault and the Puysegur Fault; and
- seafloor spreading fabric with three distinct orientations on oceanic crust west of the Puysegur Trench.

The Kermadec-Hikurangi Margin

East of New Zealand, changes in structure and sedimentation along the PAC-AUS plate boundary reflect transitions from intra-ocean subduction at the Kermadec Trench, to subcontinental subduction at the Hikurangi Trough, to continental collision of the Chatham Rise. These changes also indicate relative plate motion from a 60° angle across the Kermadec Trench to a more oblique angle (20°) along the southern Hikurangi Trough. Here the convergence rate southward also decreases from 6 to 3.9 cm/yr [*De Mets,* 1990]. On the Pacific plate, the 10–15 km thick Hikurangi Plateau, which has areas of abundant seamounts and sediment-filled troughs, is subducted westward at the southern Kermadec Trench and Hikurangi Trough [*Davy,* 1992]. On the Australian plate, south of the Kermadec island arc, the eastern edge of the New Zealand continental crust is a compressed wedge of mid-Cenozoic slope sediments, with local outgrowth of an accretionary wedge of off-scraped trench sediments [*Lewis and Pettinga,* 1993].

The GEODYNZ-SUD cruise focused on the above-mentioned transition zones of the Kermadec-Hikurangi margin (Figure 1) to clarify the relationships between subduction and strike-slip motion and to assess the impact of seamount and scarp subduction on the evolution of the margin.

Observations in the northern part of the survey area suggest that the 1000-m-high scarp forming the northern edge of the Hikurangi Plateau has swept southward along the trench. North of the scarp-trench junction, the sweep has left a collapsing inner trench wall that is offset 15 km westward from the trench to the south. South of the junction, the Hikurangi Plateau has uplifted the Kermadec forearc and trench axis by 1.5 km to form a series of narrow en echelon, sediment-starved basins (Figure 2). On the northern Hikurangi Plateau, there are several previously unrecognized, highly reflective, presumably volcanic seamounts and ridges trending N140°–168°E and ranging up to 1000 m high. Some of the seamounts lie in front of a newly recognized indentation of the margin that is 270 km long (37°45'to 40°S) and up to 25 km wide. This indented margin has an abnormally steep inner slope and abundant slump and collapse features, suggesting extensive tectonic erosion of the margin by seamount collisions. This process causes slope failures that feed the Hikurangi Trough with avalanche deposits. These deposits, ponding in the Hikurangi Trough, fail to reach the Kermadec Trench because they are impeded by a ridge at 37°45'S.

We recognized strike-slip faulting, previously known only onshore, at least 70 km east of the shore. This faulting appears to be widespread along the northern and southern Hikurangi margins that accommodate part of the oblique subduction of the Hikurangi Plateau (Figure 2). In the north, the evidence for strike-slip faults includes scarps and morphologic lineaments that define northward diverging horse tail tectonic patterns near 37°S and near 40°S.

In the south, dextral strike-slip is evident as offset ridges with small "pull apart" basins behind the accretionary wedge. In contrast, at the southern end of the accretionary wedge, the new data show extremely linear, back-tilted thrust ridges, striking 45° to the plate convergence direction. Thus a geographic separation between strike-slip faulting and thrusting suggests some strain partitioning across the margin. The compressive component is taken up mainly within off-scraped Plio-Pleistocene trench sediment of the accretionary wedge. Behind this wedge the Cenozoic slope sediment takes up much of the strike-slip component of the strain.

At the southern end of the accretionary wedge, where the margin is almost parallel to the convergence direction, strike-slip faults in the upper margin converge southwestward in a horse tail tectonic pattern. Farther south, in the zone of continental collision, the margin is deformed mainly by compression. On the adjacent land a wide zone of transpression links south with the Alpine Fault that extends to Fiordland.

The Fiordland-Puysegur Margin

Southwest of New Zealand, the Australian plate is subducted eastward along the Pacific-Australian plate boundary. The GEODYNZ-SUD study focused on the structural transitions between the Fiordland continental margin (trending N30°–45°E) at the southern end of the Alpine Fault, the continent-to-ocean transition zone of the Puysegur Bank (trending N10°–15°E), and the N20°–25° E trending Puysegur Ridge (the northern part of the Macquarie Ridge Complex) and Puysegur Trench (Figures 1 and 3). Along these segments, the relative plate motion is very oblique (20°–40°) to the deformation front, and the convergence rate is uniform (3.7–3.2 cm/yr) [*De Mets et al.,* 1990]. On the lower plate, the Resolution Ridge (Figure 3) is thought to separate the Cretaceous-Paleocene Tasman Sea oceanic crust (to the northwest) from a southeastern Eocene-Oligocene wedge of Indian Ocean oceanic crust [*Weissel et al.,* 1977]. On the upper plate, the dextral transpressive Alpine fault [*Wellman,* 1953] is thought to lie along the continental shelf of Fiordland (Figure 1). Beneath Fiordland, an 80°SE dipping Benioff zone [*Smith and Davey,* 1984] defines the morphology of the subducting Australian plate. South of Fiordland, although subduction is marked by the Puysegur Trench and a single, Quaternary andesitic volcano, there is no clear Benioff zone. Focal mechanisms show both strike-slip and thrust type deformation [*Anderson et al.,* 1993].

New data collected in the area adjacent to Fiordland show that submarine canyons, which incise the upper margin west of the presumed Alpine Fault trace, appear to be laterally offset from the mouths of fiords. This offset indicates recent dextral strike-slip displacement along the upper margin. Several linear fault scarps, (presumably strike-slip), splay southwestward in horse-tail fashion across the continental slope (Figure 3). These scarps splay away from the presumed main trace of the Alpine fault and appear to reach the subduction deformation front. This pattern suggests that the Fiordland margin is obliquely segmented into continental strike-

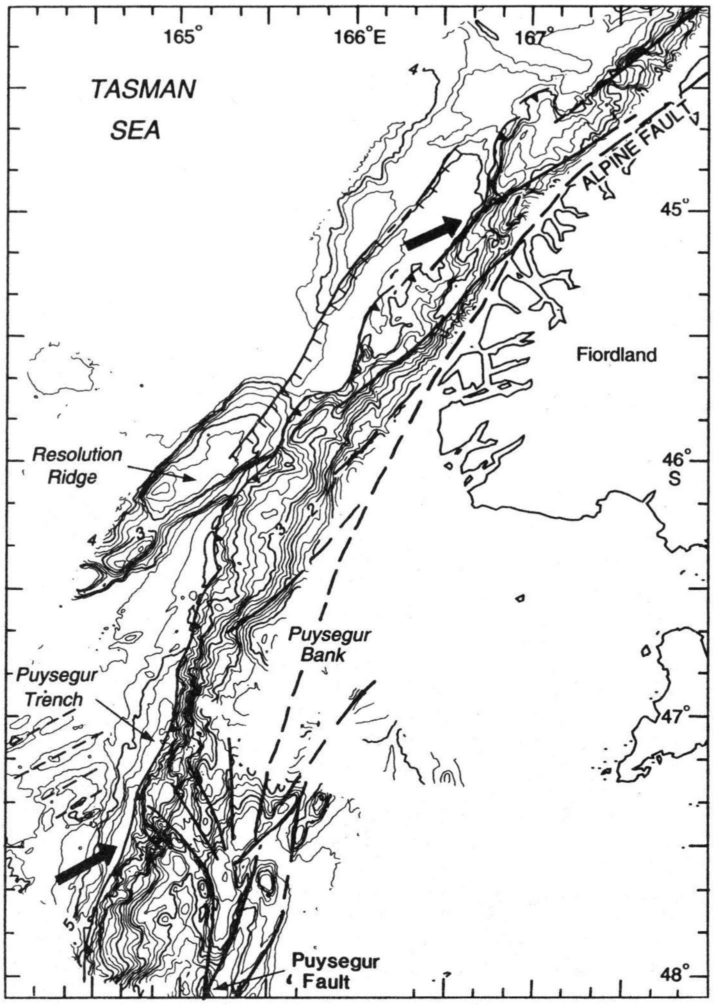

Fig. 3. Generalized multibeam bathymetric map (contour interval 250 m) of the Fiordland-Puysegur margin. Faults splay southwestward away from the presumed offshore trace of the Alpine Fault, and south of the Puysegur bank, the strike-slip, fan-shaped pattern of faults merge southward with the Puysegur Fault; thick solid lines = faults; sawtooth line = subduction front; short dashed lines = N60°E trending oceanic fabric; large arrow = PAC-AUS plate convergence direction.

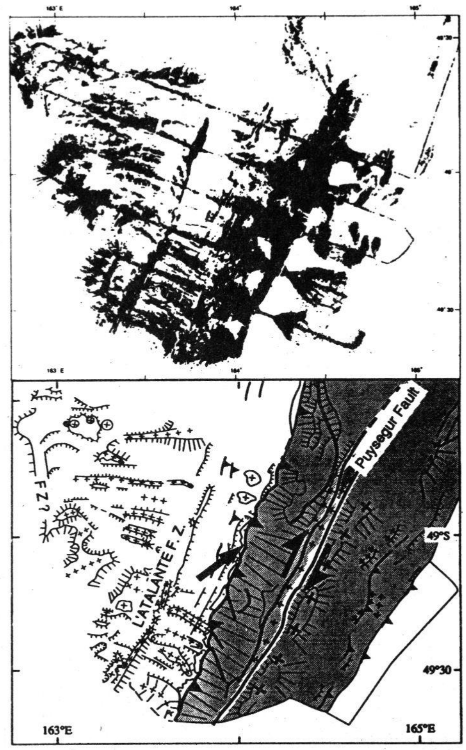

Fig. 4. (top) Side scan sonar imagery (high reflectivity is shown as black), and (bottom) structural interpretation of the Puysegur Fault, L'Atalante Fracture Zone and oceanic fabrics (trending N120° and N85°E) west of the Puysegur Trench; the Puysegur Ridge is shaded; crosses = bathymetric highs; large sawtooth line = thrusting front; small sawtooth line = reverse faults; lines with ticks = scarps or normal faults; large arrow = plate convergence [De Mets et al., 1989]; *double arrow = strike-slip motion along the Puysegur Fault.*

slip slivers that are underthrust by the Australian plate.

South of Puysegur Bank, in the Puysegur Ridge, the tectonic pattern suggests that strike-slip is distributed throughout a fan-shaped, fault-sliver, valley-and-ridge terrain on the overriding plate. These faults converge south of latitude 48° S to form a sharply localized, linear zone of deformation parallel to the ridge about 55 km east of the trench (Figure 3). The narrow shear zone continues southward into the summit region of the very linear, highly reflective Puysegur Ridge as an axial valley, trending N25°E, 20–33 km east of the trench (Figure 4). This perched valley is a series of elongated troughs that relay and locally overlap along the strike of the ridge, isolating uplifted and downthrown blocks.

We believe that most, if not all, of the strike-slip motion on this part of the plate boundary takes place along the axial valley. This valley represents the trace of a major fault that we named the Puysegur Fault. The overall tectonic pattern at the transition between the Fiordland margin and the Puysegur Ridge suggests that a relay zone of splay strike-slip faults links the continental Alpine Fault to the oceanic Puysegur Fault.

Evidence for eastward subduction, local tectonic accretion and tectonic erosion also stems from the newly acquired data. At the front of the continental strike-slip slivers, east of Fiordland, small accretionary lobes extend into the trench, a 10–20 km wide and 4000-m-deep sediment-filled basin. The outer trench wall is deformed by Recent trench-parallel normal faults caused by plate flexure. The Resolution Ridge, a series of en echelon blocks, crosses the trench opposite the southern end of Fiordland. South of the ridge the inner trench shows possible damage from previous subduction of a segment of the ridge. From latitude 47°S, the Puysegur Trench extends southward as an en echelon, narrow, flat-bottomed trough deepening from 5500 to 6200 m near 48°S and shallowing farther south to 5200 m where the trench disappears. The inner trench wall from 47° to 48°S shows evidence for indentation and slope failures suggesting frontal tectonic erosion where the Puysegur Ridge is the widest. Farther south of 48°30', where the ridge narrows and shoals to 125 m, the inner trench wall becomes steeper and regular. The southward changes—narrowing and shallowing of the ridge, its along-strike morphologic change and the disappearance of the trench—may be an indication of the process of subduction initiation in this region suggested by *Ruff et al.* [1989].

The clear spreading fabric on the oceanic Australian plate (including fracture zones such as L'Atalante Fracture Zone) containing three different spreading directions was an unexpected discovery. The fabric trends N120°E near 49°30S, N85°E near 48°30S (Figure 4) and N60°E near 47°S (Figure 3, lower left). The N60°E trend is parallel to the late Eocene-early Oligocene magnetic anomalies farther southwest that were recognized by *Weissel et al.* [1977], but the trends we observed are new discoveries. We have not identified any triple junction. These trends appear to represent either discrete or gradual changes of spreading direction, at least in this region, during the Cenozoic.

Scientific Party

J.-C. Audru, B. Mercier de Lepinay, M. Popoff, E. Ruellan, and M. Sosson, IG, Nice, France; P. Barnes, NIWA, Wellington, New Zealand; G. Lamarche, J.-F. Lebrun, B. Pontoise, and B. Toussaint, ORSTOM, Villefranche s/mer, France; S. Calmant and B. Pelletier, ORSTOM, Noumea, New Caledonia; F. Chanier and J. Ferriere, University of Lille, France; E. Chaumillon, Laboratoire de Geodynamique, Villefranche s/mer, France; M. Coffin UTIG, Austin, Tex.; B. Davy and C. Uruski, IGNS, Wellington, New Zealand; D. Christoffel, Victoria University, Wellington, New Zealand; S. Lallemand, University of Montpellier, France; A. Mauffret, CNRS, Paris, France; A. Orpin and R. Sutherland, Otago University, New Zealand

Acknowledgments

We thank INSU, ORSTOM, Foundation for Research, Sciences & Technology of New Zealand, IGNS, NIWA and the Ministry of French Foreign Affairs for funding and supporting this collaborative work, IFREMER for providing R/V *L'Atalante* ship time and equipment, and GENAVIR officers, technicians and crew.

References

Anderson, H., T. Webb and J. Jackson, Focal mechanism of large earthquakes in the South Island of New Zealand; Implications for the accommodation of Pacific-Australia plate motion, *Geophys. J. Int., 115,* 1032, 1993.

Davey, F. J., M. Hampton, J. Childs, M. A. Fisher, K. B. Lewis and J. R. Pettinga, Structure of a growing accretionary prism, Hikurangi margin, New Zealand, *Geology 14,* 663, 1986.

Davy, B. M., The influence of subducting plate buoyancy on subduction of the Hikurangi-Chatham Plateau beneath North Island, in *Proceedings of the Halbouty Conference,* edited by J. S. Watkins, F. Zhiqiang and K. J. McMillen, 75 pp., American Association of Petroleum Geologists, Tulsa, Okla., 1992.

De Mets, C., R. G. Gordon, D. F. Argus and S. Stein, Current plate motions, *Geophys. J. Int., 101,* 425, 1990.

Lewis, K. B. and J. R. Pettinga, The emerging, imbricate frontal wedge of the Hikurangi margin, in *Basins of the Southwest Pacific: Sedimentary Basins of the World,* vol. 3, edited by P. F. Ballance, 1993.

Ruff, L. J., J. W. Given, C. O. Sanders, and C. M. Sperber, Large earthquakes in the Macquarie Ridge Complex: Transitional tectonics and subduction initiation, *Pure and Applied Geophysics, 128,* 72, 1989.

Smith, E. C. C. and F. J. Davey, Joint hypocenter determination of intermediate depth earthquakes in Fiordland region, New Zealand, *Tectonophysics, 104,* 127, 1984.

Weissel, J. F., D. E. Hayes and E. M. Herron, Plate tectonics synthesis: The displacement between Australia, New Zealand, and Antarctica since the late Cretaceous, Mar. *Geology, 25,* 231, 1977.

Wellman, H. W., Data for the study of Recent and late Pleistocene faulting in the South Island of New Zealand, N. Z., *J. Sci. Technol, B34,* 270, 1953.

Pairing of Radar Instruments on Satellites Could Provide Optimal Mapping of Sea Surface Winds

PAGE 3

Jin Wu

Scientists pairing two radar instruments with different sensitivities to ripples on the ocean surface may be able to measure the entire range of sea surface wind speeds—vital parameters that affect climate and the ocean environment.

Ocean ripples detected via remote radar sensing are effective tracers of sea surface wind velocity [*Woiceshyn et al.*, 1986; *Wu,* 1990b]. The scatterometer, which detects the scattering of radar waves by ripples on the sea surface, is deployed on Earth-orbiting satellites to map wind velocities over the world's oceans. The scatterometer/wind anemometry relationship has been derived from data collected mainly under intermediate wind velocities.

Radar returns for the scatterometer are erratic, however, at low wind speeds [*Woiceshyn et al.*, 1986], which prevail over the oceans [*Harrison,* 1989]. Winds are especially light over tropical regions [*Sadler et al.*, 1987], where most of the heat transfer from oceans to the atmosphere takes place. In these regions, precise wind measurements are essential for evaluating long-term climate changes. The altimeter, which operates on the basis of specular reflections from ripples, performs most effectively at the low wind speeds in these areas [*Witter and Chelton,* 1991; *Wu,* 1994]. This sensor was designed primarily for measuring sea-surface elevations [*Chelton et al.*, 1989].

Jin Wu, Air-Sea Interaction Laboratory, Graduate College of Marine Studies, University of Delaware, Lewes, DE 19958

The altimeter may be used for measuring low speed winds ($U < 5$ m s^{-1}) and the scatterometer, for winds of higher velocity. The scatterometer can detect the wind direction effectively at all wind speeds from the pattern of its returns at various azimuth angles [*Wu,* 1990a].

Remote Sensing of Sea-Surface Winds

Scatterometer The Seasat A scatterometer system (SASS) employed for measuring sea surface wind speeds was a 14.6-GHz (2.1-cm wavelength) active microwave radar. Radar sea returns at medium incidences follow the first-order Bragg scattering, wherein the ocean wave number is related to the radar wave number and the angle of microwave incidence.

Altimeter The backscattering of radiation at small incidences from the sea surface is primarily specular reflection—e.g., reflection of microwaves from sea surface ripples that are small compared with the wavelength of the incident radiation. In their classical study of sun glitters on the sea surface, *Cox and Munk* [1954] calculated the variation of mean-square slope of ocean ripples with wind velocity. The radar returns are, of course, from ripples over the illuminated area, but only those with length longer than the radar wavelength can contribute to specular returns. From Cox and Munk's results, *Wu* [1990a] deduced the mean-square slopes contributed by wave components with their length longer than 2.5 cm. The X band radar used for the Geosat altimeter had a wavelength of about 2.16 cm, differing only slightly from the wavelength discussed above. *Wu* [1994] derived an analytical altimeter wind algorithm using these spectrally resolved results of normally distributed ripple slopes. Wind speeds calculated using the algorithm compared favorably with those tablulated with the algorithm proposed by *Witter and Chelton* (1991) for Seasat altimeter data, except at very light winds ($U_{10} < 0.3$ m s^{-1}).

Detected Trends at Low Winds

Scatterometer *Woiceshyn et al.* [1986] examined the scatterometry wind algorithm on the basis of in situ wind measurements from the ocean platform during the Joint Air-Sea Interaction Experiment (JASIN) in the North Atlantic Ocean, and from buoys operated by the National Data Buoy Ofice (NDBO) off the Gulf coasts and in the North Atlantic and Pacific oceans. This comparison, organized into intervals of increasing wind speed, included 500 pairs of SASS/JASIN measurements and 100 pairs of SASS/NDBO measurements.

The SASS wind velocities, expressed in terms of the radar cross section, are compared to the in situ wind velocities at the standard anemometer height in Figure 1 [*Woiceshyn et al.*,1986]. At high winds, scatterometer returns increase linearly with the logarithm of wind velocity. However, this relationship breaks down at about $U_{10} < 6$ m s^{-1} for JASIN results, and at about $U_{10} < 4$ m s^{-1} for

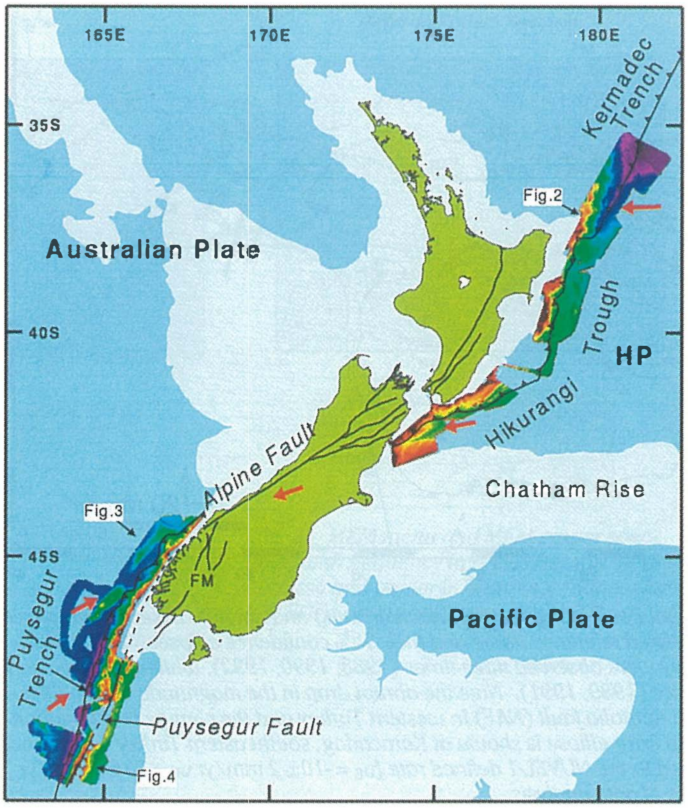

Fig. 1. Map of the areas surveyed during the Geodynz-Sud cruise of the R/V L'Atalante *along New Zealand's active margins with linearly color-coded swath bathymetry; red arrows = PAC-AUS plate convergence direction* [De Mets et al., 1990]; *HP = Hikurangi Plateau; FM = Fiordland Margin; sawtooth lines = subduction fronts; heavy lines = major strike-slip faults; light blue = continental rocks, depth <1.5 km; and dark blue = seafloor depth >1.5 km.*